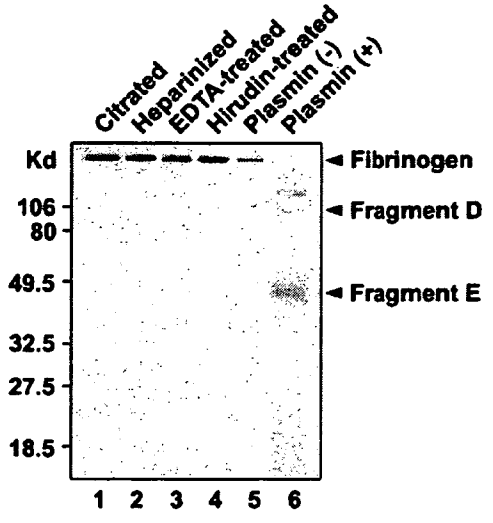

Figure 2 Fibrinogen is not cleaved by patient plasma. Non-labeled fibrinogen (30 μM) and 300 nM ^{125}I-fibrinogen were incubated with citrated (lane 1), heparinized (lane 2), EDTA-treated (lane 3), or hirudin-treated plasma (lane 4) from the first patient at 37 °C for 1 h in the presence of 1 μM plasminogen. Non-labeled fibrinogen (30 μM) and 300 nM ^{125}I-fibrinogen was treated similarly without (lane 5) or with 10 nM plasmin (lane 6). Each sample was analyzed by 10–15% gradient SDS-PAGE under non-reducing conditions followed by autoradiography.

(Muto Pure Chemicals, Osaka, Japan). These samples were also treated with the immunoperoxidase procedure as described elsewhere. Anti-human von Willebrand factor rabbit IgG (NeoMarkers, Fremont, CA, USA), anti-human thrombomodulin mouse IgG (Daiichi Fine Chemicals, Toyama, Japan), anti-human tissue factor pathway inhibitor (TFPI) mouse IgG (American Diagnostica, Greenwich, CT, USA), anti-human annexin 2 rabbit IgG (Santa Cruz Biotechnology), anti-human CD31 mouse IgG (Dako, Carpinteria, CA, USA), anti-human t-PA rabbit IgG [18], anti-human u-PA rabbit IgG (Technoclone, Vienna, Austria), anti-human urokinase type plasminogen activator receptor (u-PAR, Neomakers) mouse IgG, and anti-human pancytokeratin 7 or 20 mouse IgG (Dako) were used as primary antibodies. Sections were incubated with primary antibodies at the appropriate concentrations (1 to 10 μg/mL) in phosphate-buffered saline (PBS) containing 0.05% Triton X-100 and 1% bovine serum albumin (BSA) for 16 h at 4 °C. After washing extensively, each sample was incubated with the horseradish peroxidase conjugated secondary antibodies at the appropriate concentrations (10 μg/mL anti-mouse IgG or 50 μg/mL anti-rabbit IgG antibodies) in PBS with 1% BSA for 1 h at 25 °C. After washing again, the immunoreactive sites were visualized with hydrogen peroxide and diaminobenzidine followed by counter staining with hematoxylin. Control sections were incubated with 5 μg/mL of non-immune isotype-matched mouse IgGs or 10 μg/mL rabbit IgG (Dako) instead of the primary antibodies, respectively.

Immunofluorescence analysis

Cultured cells on Lab-Tek chamber slides (Nalge Nunc, Naperville, IL, USA) were washed in PBS, fixed with 1% paraformaldehyde for 20 min at 25 °C, and

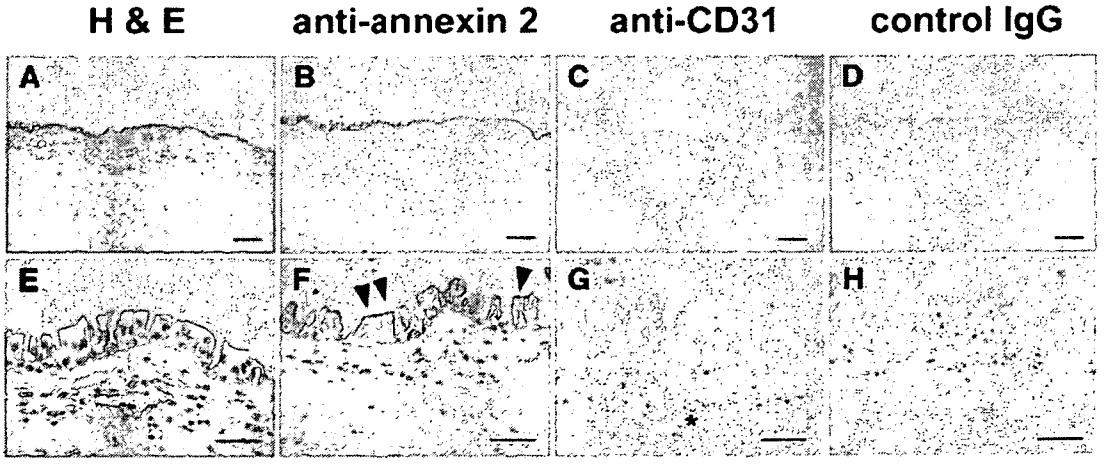

Figure 3 Morphological and immunohistochemical analyses of pulmonary arteries' vascular intimal carcinomatosis. Pulmonary arteries' vascular intimal carcinomatosis was stained with hematoxylin and eosin (A and E), and then immunostaining was performed with anti-human annexin 2 (B and F), anti-human CD31 (C and G), or control IgG (D and H). Arrowheads show monolayers of cuboidal tumor cells that stain positive for annexin 2 at the margin of the vascular intimal carcinomatosis. The asterisk indicates a normal small blood vessel in the pulmonary arterial vascular wall. Scale bars represent 100 μm in A–D and 50 μm in E–H.

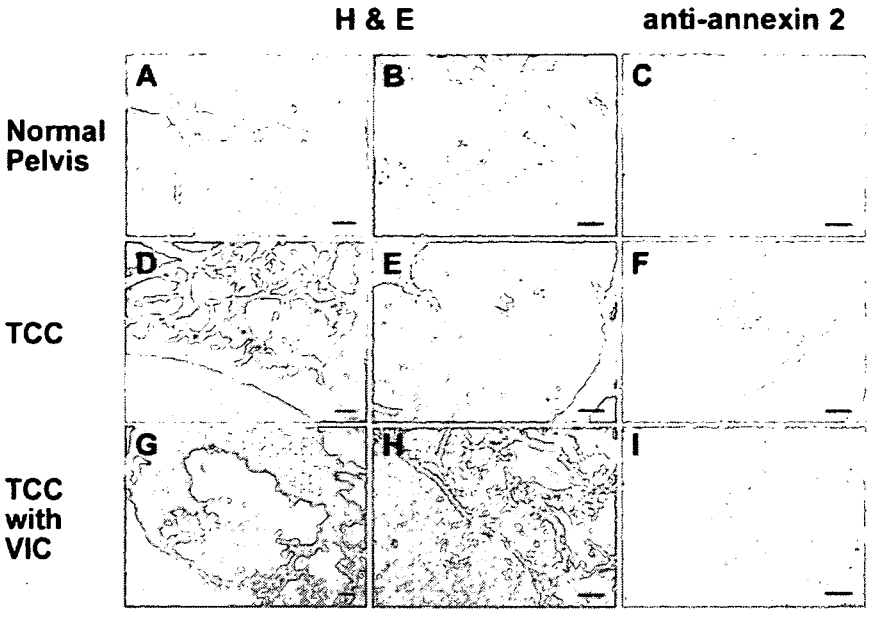

Figure 4 Morphological and immunohistochemical analyses of renal pelvic transitional cell carcinoma. Normal pelvis (A and B), transitional cell carcinoma (D and E), and transitional cell carcinoma with pulmonary arteries' vascular intimal carcinomatosis (G and H) were stained with hematoxylin and eosin. Immunostainings with anti-human annexin 2 were performed in normal renal pelvis (C), transitional cell carcinoma (F), and transitional cell carcinoma with pulmonary arteries' vascular intimal carcinomatosis (I). TCC: transitional cell carcinoma, VIC: vascular intimal carcinomatosis. Scale bars represent 500 μm in A, D, and G; and 100 μm in B, C, E, F, H, and I.

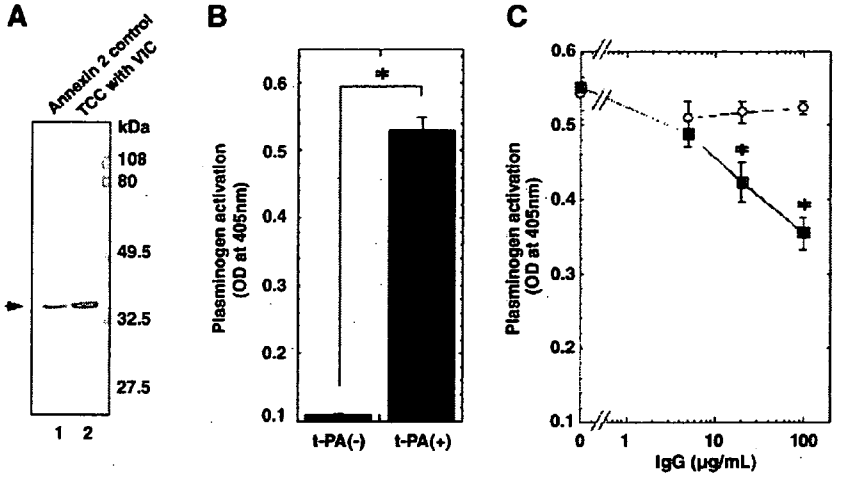

Figure 5 Annexin 2 expression and plasminogen activation in transitional cell carcinoma with vascular intimal carcinomatosis. (A) The cell membrane extracts isolated from transitional cell carcinoma cells with vascular intimal carcinomatosis were analyzed with 10% SDS-PAGE followed by immunoblotting with anti-annexin 2 IgG under reducing conditions. Lane 1, annexin 2 control; lane 2, transitional carcinoma with vascular intimal carcinomatosis. (B) Lys-plasminogen (100 nM) was preincubated in the presence of transitional cell carcinoma cells with vascular intimal carcinomatosis at 25 °C for 1 h. S-2251 was then added (500 nM) together with t-PA (10 nM), and the absorbance at 405 nm was measured for 30 min. (C) Varying concentrations (0–100 μg/mL) of anti-annexin 2 IgG (closed squares) or control IgG (open circles) were preincubated with transitional cell carcinoma cells with vascular intimal carcinomatosis at 25 °C for 1 h, and then incubated with Lys-plasminogen (100 nM) at 25 °C for 1 h. The plasminogen activation was monitored by measuring the absorbance at 405 nm at 25 °C after addition of t-PA (10 nM) and S-2251 (500 nM). Values are each the mean ± S.D. of 5 samples in each group. *$P<0.01$ when compared to each group. TCC: transitional cell carcinoma, VIC: vascular intimal carcinomatosis.

blocked against nonspecific binding with PBS containing 0.05% Triton X-100 and 2% BSA for 1 h at 25 °C. After the incubation, samples were washed with PBS containing 0.05% Triton X-100 and 1% BSA, followed by incubation with 10 μg/mL of fluorescein isothiocyanate (FITC)-conjugated anti-annexin 2 IgG (BD Biosciences, San Jose, CA, USA) for 1 h at 25 °C. After washing, samples were mounted with fluorescent mounting medium (Dako) and processed slides were examined under a Nikon E800M fluorescent microscope (Nikon, Tokyo, Japan).

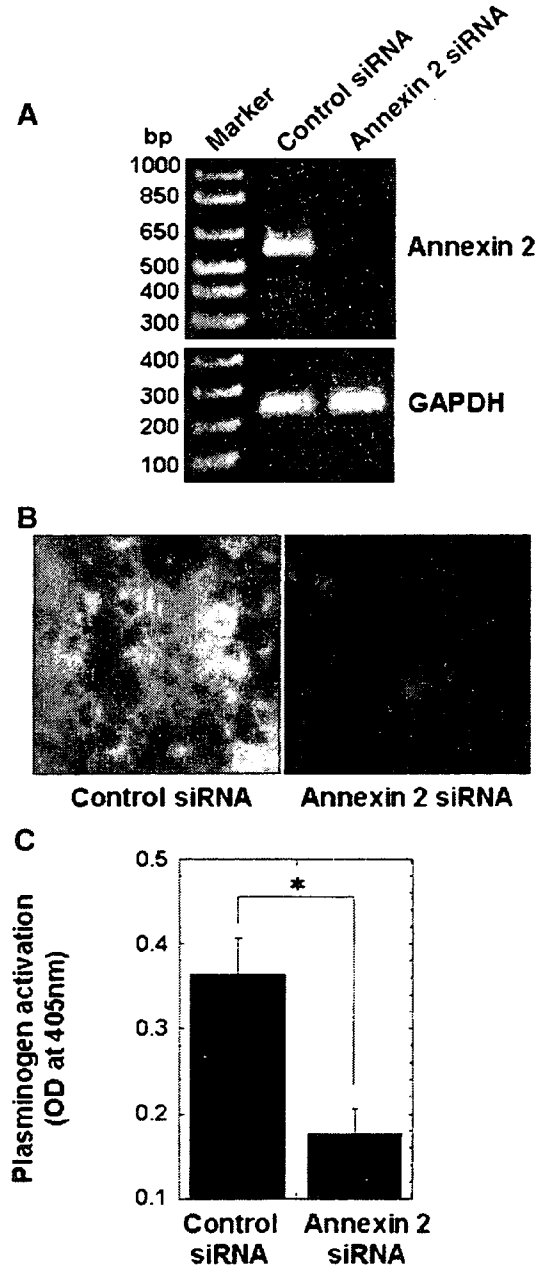

Statistical analysis

The statistical difference was determined by the two-sided Student's *t*-test. A difference with $P<0.05$ was considered significant.

Results

Fibrinogenolysis with transitional cell carcinoma

All patients with transitional cell carcinoma showed evidence of consumption coagulopathy and hyperfibrino(geno)lysis: low plasma fibrinogen concentration and high levels of fibrinogen and fibrin degradation products without marked elevation of D-dimer nor thrombocytopenia (Table 1). Factor XIII activities were also normal in these cases (data not shown). Despite continuous infusion of fresh frozen plasma, and/or fibrinogen concentrates, these patients had overt bleeding including intramuscular hematoma, intraperitoneal and intracranial bleeding. To address how hyperfibrino(geno)lysis occurred in these patients, we immunopurified fibrinogen-derived proteins from their plasma using anti-fibrinogen polyclonal antibody-Sepharose. Plasmic digestion of normal fibrinogen in the presence of $CaCl_2$ generates D fragment, which consists D1A/γ, D1/γ, and D1/β, and E fragment in a time-dependent manner (Fig. 1A: lanes 4–6 and 11–13). Plasmin digestion of cross-linked normal fibrin results in the fragments D-dimer and E as the main products (Fig. 1A: lanes 2, 3, 9 and 10). When

Figure 6 Knockdown of annexin 2 gene expression by siRNA inhibits plasminogen activation in transitional cell carcinoma with vascular intimal carcinomatosis. (A) The isolated transitional cell carcinoma cells with vascular intimal carcinomatosis were transfected with annexin 2 or control siRNA as described in Materials and methods. After 30 h, total RNA was extracted from each transfectant, and RT-PCR analysis for annexin 2 or GAPDH mRNA expression was performed. Amplified products were analyzed on 1.5% agarose gels followed by ethidium bromide staining. (B) The annexin 2 or control siRNA transfected transitional cell carcinoma cells with vascular intimal carcinomatosis were immunohistochemically stained with FITC-conjugated anti-annexin 2 IgG and examined under a fluorescent microscope (magnification: ×400). (C) The annexin 2 or control siRNA transfected transitional cell carcinoma cells with vascular intimal carcinomatosis were subjected to the assay for plasminogen activation as described above. Values are each the mean ± S.D. of 5 samples in each group. *$P<0.01$ when compared to each group.

immunopurified products from patients' plasma were analyzed, several bands appeared that corresponded with D fragment under non-reducing conditions and with D1A/γ, D1/γ, and D1/β under reducing conditions (Fig. 1A: lanes 7 and 14). D1A/γ and D1/γ polypeptides also stained positively with JIF-23 monoclonal antibody that recognizes the NH_2-terminal conformation of the fragment D species [13] (Fig. 1B: lane 7). A small amount of γ–γ dimer remnant fragments formed during plasmic digestion of cross-linked fibrin were also noted. These findings suggest that systemic fibrinogenolysis by plasmin occurred in these patients with transitional cell carcinoma.

Patient plasma is unable to degrade fibrinogen

We initially suspected that the activation of plasminogen in our patients was caused by a plasminogen activator(s) in their plasma. ^{125}I-fibrinogen was incubated with patient plasma in the presence of plasminogen and then analyzed by SDS-PAGE and subjected to autoradiography. The results showed that citrated, heparinized, EDTA-treated, or hirudin-treated patient plasma could not degrade fibrinogen (Fig. 2). We also investigated plasminogen activators of the patients' plasma by fibrinautography, however, there were no identifiable levels of plasminogen activators in their samples (data not shown). Moreover, the expected plasminogen to plasmin conversion did not occur after incubation with the patients' plasma samples as judged by an amidolytic assay using a substrate specific for plasmin or by SDS-PAGE followed by immunoblotting with anti-plasminogen polyclonal antibodies (data not shown).

Pulmonary metastases of transitional cell carcinoma show vascular intimal carcinomatosis and express annexin 2

For each patient, autopsy revealed a previously unknown carcinoma with metastases and with distinct tumor-related angiopathic lesions in large pulmonary arteries. The carcinoma cells had abundant eosinophilic cytoplasm that had diffusely replaced the endothelium and expanded onto the intima of pulmonary arteries without occlusion of the vessels (Fig. 3A and E). There was no fibrous intimal proliferation or granulomatous inflammation within the subendothelial layers. Interestingly, the surfaces of the tumor cells were free from thrombotic matter, but some thrombi adhered to lesions that were deficient of endothelium or carcinoma cells (data not shown). These observations are consistent with vascular intimal carcinomatosis [5,6]. Immunohistochemically, the carcinoma cells stained positive for cytokeratins (data not shown), but were negative for endothelial cell-related antigens such as von Willebrand factor and CD31 (Fig. 3C and G). Since the clinical course included hemorrhagic disorders of unknown cause, we investigated expression of regulatory factors of the blood coagulation system in these tumors. The cells showed slightly positive staining for TFPI, thrombomodulin and t-PA, also they weakly expressed u-PA and its receptor (data not shown). Surprisingly, the spreading intimal tumors showed strong staining for annexin 2, especially at the tumor surface (Fig. 3B and F). The primary lesions showed papillary tumors with invasion to the pelvic mucosa, and they were histologically revealed to be transitional cell carcinoma (Fig. 4G and H). Interestingly, annexin 2 expression was observed in these neoplastic cells (Fig. 4I), while normal pelvic mucosa and transitional cell carcinoma without vascular intimal carcinomatosis were devoid of staining (Fig. 4A–C and D–F, respectively).

Annexin 2 expression and plasminogen activation in transitional cell carcinoma with vascular intimal carcinomatosis

We isolated carcinoma cells from a surgical specimen of the first case and analyzed cellular expression of annexin 2. As shown in Fig. 5A, annexin 2 was detected in elutes from these transitional cell carcinomas by Western blot analysis using anti-annexin 2 IgG. To address how annexin 2 on the transitional cell carcinomas relates to the induction of hyperfibrino(geno)lysis, we assessed the ability of these tumor cells to activate plasminogen. In the absence of t-PA, the plasmin generation was not enhanced by the isolated carcinoma cells. In contrast, when t-PA was added along with the tumor cells, plasminogen activation was significantly increased as compared with that with the tumor cells alone (Fig. 5B). The plasmin generation on the transitional cell carcinomas was inhibited by anti-annexin 2 IgG to 64.1% ($P<0.01$) of that observed when these tumor cells were incubated with control IgG (Fig. 5C). To further analyze the role of annexin 2 on the tumor cells surface in the t-PA-mediated activation of plasminogen, the transitional cell carcinomas were transfected with oligonucleotides containing either the annexin 2 siRNA or control siRNA. As expected, the annexin 2 mRNA expression was effectively suppressed in the annexin 2 siRNA transfected

carcinoma cells (Fig. 6A). Moreover, the surface expression of annexin 2, as assessed by immunofluorescence microscopy, was strongly inhibited in the transitional cell carcinomas transfected with annexin 2 siRNA (Fig. 6B). The plasminogen activation on the transfectants with annexin 2 siRNA was significantly reduced as compared with that of the control siRNA transfectants (Fig. 6C). These results suggest that annexin 2 on the surface of transitional cell carcinoma with vascular intimal carcinomatosis has an important role in plasmin generation.

Discussion

Fibrinogenolysis, in which circulating fibrinogen molecules are proteolyzed and severe bleeding may develop, is a rare pathophysiological condition [19] and its underlying mechanism has remained unclear. Many reports have shown that systemic hyperfibrino(geno)lysis can induce a bleeding disorder through the release of plasminogen activators from cancer tissue [7–10,20]. The clinical features of our cases with transitional cell carcinoma included hemorrhagic diathesis, which was thought to result from severe hypofibrinogenemia (Table 1). We immunopurified fibrinogen-derived proteins from these patients' plasmas with anti-fibrinogen IgG and then analyzed them by immunoblotting using JIF-23 antibody that specifically recognizes the NH_2-terminus of fragment D [13]. Fragment D, which was confirmed to contain D1A and D1, and fragment E were the main products with small amounts of fragment DD being present (a γ–γ dimer remnant observed under reducing conditions) (Fig. 1). These results suggest that systemic fibrinogenolysis by plasmin could be a primary cause of the hypofibrinogenemia in these patients, although consumption coagulopathy might exist in these cases.

Pathological examination of autopsy specimens revealed that metastatic transitional cell carcinoma had diffusely replaced the endothelium and expanded onto the intima of pulmonary arteries without occlusion of the vessels (Fig. 3). These pathological conditions are described as vascular intimal carcinomatosis [5,6]. Transitional cell carcinoma is known to spread along large structures such as the ureter and major vessels [21,22]. However, once any malignant neoplasm expands onto the pulmonary vessels, the risk arises of widespread obstruction of pulmonary arteries by the tumor cells [23,24]. On the other hand, several reports show that tumor emboli do not necessarily occlude affected vessels, but induce both local activation of blood coagulation and fibrocellular intimal proliferation of small arteries and arterioles, which is known as tumor thrombotic angiopathy [25–27]. We showed that the surfaces of the expanded tumor cells were devoid of thrombotic materials and that those thrombi were localized only on the areas deficient of endothelial cells or carcinoma cells (Fig. 3), suggesting that these tumor cells have some mechanism that allows then to escape from the host thrombus formation system.

Tagnon et al. demonstrated that plasma from patients with prostatic cancer could accelerate fibrin degradation in vitro [28]. In the current study, however, our patients' plasma samples per se had no observable plasminogen activator or fibrinogen degradation activity (Fig. 2). Interestingly, immunostaining for annexin 2 in the spreading intimal tumors on pulmonary arteries demonstrated diffuse cytoplasmic staining and strong signals at the tumor cell surface (Fig. 3). These results might be compatible with the previous reports that annexin 2 is an intracellular protein located on the cytosolic face of the plasma membrane and that annexin 2 translocates to the extracellular membrane surface in activated endothelial and some tumor cells [29,30]. Annexin 2 is thought to have a thromboregulatory role by enhancing t-PA-dependent formation of plasmin on the endothelial cell surface [11,31–34]. We demonstrated that the isolated transitional cell carcinoma cells expressed annexin 2 mRNA and its protein. In addition, these tumor cells possessed annexin 2 related plasmin generation activity that was significantly inhibited by both anti-annexin 2 IgG and annexin 2 siRNA transfection (Figs. 5 and 6). The high level of annexin 2 expression on acute myeloid leukemia cells appeared to increase the production of plasmin on their surfaces and may contribute to a hemorrhagic disorder [12,35,36]. Once plasmin is formed or binds onto the cell surface, it is protected from its primary inhibitor α2-plasmin inhibitor so that local proteolysis could be achieved even in an environment rich in plasmin inhibitors [37]. Thus, it is possible that dysregulated expression of annexin 2 on the surface of transitional cell carcinoma cells, lining the vascular lumen and replacing normal endothelium, might lead to uncontrolled production of plasmin. This, along with u-PA and the expression of its receptor, dysregulated expression of annexin 2 may shift the hemostatic balance toward overt bleeding. Annexin 2 exists at the cell surface as a complex with p11 (S100A10) that is known to promote plasminogen activation [38,39]. We found that our transitional cell carcinoma showed weakly positive staining for p11 (data not shown), consequently p11 might play some roles in hemorrhagic disorders in vascular intimal carcinomatosis.

Not only normal pelvic mucosa but also transitional cell carcinoma without vascular intimal carcinomatosis did not express any annexin 2 protein (Fig. 4). In contrast, our patients' transitional cell carcinoma with vascular intimal carcinomatosis showed positive staining for annexin 2 at the primary lesion (renal pelvis) and metastatic site (pulmonary artery) (Figs. 3 and 4). Several reports have shown that certain cancer cell types will mimic the activities of endothelial cells and will participate in endothelial non-angiogenic pathways [40–44]. Recently, annexin 2-deficient mice have markedly impaired postnatal angiogenesis due to failed vascular fibrin homeostasis, thrombi clearance, and activation of selected matrix metalloproteinases (MMPs) [45]. Annexin 2 on the tumor cells surface locally increases the t-PA mediated plasmin production from plasminogen. Then, the plasmin might activate pro-MMPs, such as MMP2 and MMP13, to active MMPs that induce extracellular matrix remodeling and facilitating the tumor invasion [46]. On the other hand, the cell surface plasmin could undergo autoproteolysis to be angiostatin that mediates apoptosis of pre-existed vascular endothelial cells [47,48]. These mechanisms may serve an important role in regulating the tumor cells expansion replacing pre-existing endothelial cells on vascular intima. Thus, the presence of vascular intimal carcinomatosis appears to be correlated with annexin 2, but further studies are needed to verify this finding.

Acknowledgements

We thank Ms. Chizuko Nakamikawa, Ms. Miyuki Tezuka and Ms. Kiyono Morita for their technical assistance. We thank Dr. D. J. Stearns-Kurosawa (IdEst, Inc.) and Dr. Stephanie Jung (Kurume University, Kurume, Japan) for critical reading and editing of this manuscript.

This work was supported in part by a Grant-in-Aid for Scientific Research (#15591021 and #17591006) to SM from the Japanese Ministry of Education, Culture, Sports, Science and Technology, and by a Health and Labor Sciences Research Grant for Research to YS from the Japanese Ministry of Health, Labor, and Welfare.

References

[1] Jitsukawa S, Nakamura K, Nakayama M, Osawa A, Matsui K. Transitional cell carcinoma of kidney extending into renal vein and inferior vena cava. *Urology* 1985;**25**:310-2.

[2] Batata MA, Whitmore WF, Hilaris BS, Tokita N, Grabstald H. Primary carcinoma of the ureter: a prognostic study. *Cancer* 1975;**35**:1626-32.

[3] Fitzpatrick TM, Covelli HD, Tenholder MF. The acute and insidious onset of pulmonary metastatic transitional cell carcinoma. *Chest* 1991;**99**:498-500.

[4] Markowitz DH, Mark EJ. Case records of the Massachusetts General Hospital. Weekly clinicopathological exercises. Case 13-2002. A 43-year-old man with renal carcinoma and worsening dyspnea. *N Engl J Med* 2002; **346**:1309-17.

[5] Kobayashi H, Tamashima S, Shigeyama J, Shimizu S, Suchi T. Vascular intimal carcinomatosis: an autopsy case of unusual form of pulmonary metastasis of transitional cell carcinoma. *Pathol Int* 1997;**47**:655-7.

[6] Madoiwa S, Mimuro J, Nakamikawa C, Morita K, Sugo T, Kurihara R, et al. Establishment and characterization of SS-TCC cell line, derived from a primary hyperfibrinolysis state with vascular intimal carcinomatosis. *Blood* 2001;**98**:263a.

[7] Davidson JF, McNicol GP, Frank GL, Anderson TJ, Douglas AS. Plasminogen-activator-producing tumour. *Br Med J* 1969; **1**:88-91.

[8] Al-Mondhiry H, Manni A, Owen J, Gordon R. Hemostatic effects of hormonal stimulation in patients with metastatic prostate cancer. *Am J Hematol* 1988;**28**:141-5.

[9] Mannucci PM, Cugno M, Bottasso B, Marongiu F, Maniezzo M, Vaglini M, et al. Changes in fibrinolysis in patients with localized tumors. *Eur J Cancer* 1990;**26**:83-7.

[10] Zacharski LR, Memoli VA, Ornstein DL, Rousseau SM, Kisiel W, Kudryk BJ. Tumor cell procoagulant and urokinase expression in carcinoma of the ovary. *J Natl Cancer Inst* 1993;**85**:1225-30.

[11] Hajjar KA, Jacovina AT, Chacko J. An endothelial cell receptor for plasminogen/tissue plasminogen activator: I. Identity with annexin II. *J Biol Chem* 1994;**269**:21191-7.

[12] Menell JS, Cesarman GM, Jacovina AT, McLaughlin MA, Lev EA, Hajjar KA. Annexin II and bleeding in acute promyelocytic leukemia. *N Engl J Med* 1999;**340**:994-1004.

[13] Matsuda M, Terukina S, Yamazumi K, Maekawa H, Soe G. A monoclonal antibody that recognizes the NH2-terminal conformation of fragment D. Amsterdam: Excepta Medica; 1990. p. 43-8.

[14] Laemmli UK. Cleavage of structural proteins during the assembly of the head of bacteriophage T4. *Nature* 1970;**227**:680-5.

[15] Blake MS, Johnston KH, Russell-Jones GJ, Gotschlich EC. A rapid, sensitive method for detection of alkaline phosphatase-conjugated anti-antibody on Western blots. *Anal Biochem* 1984;**136**:175-9.

[16] Madoiwa S, Arai K, Ueda Y, Ishizuka M, Mimuro J, Asakura S, et al. A battery of monoclonal antibodies that induce unique conformations to evolve cryptic but constitutive functions of plasminogen. *J Biochem (Tokyo)* 1997;**121**: 278-87.

[17] Chomczynski P, Sacchi N. Single-step method of RNA isolation by acid guanidinium thiocyanate–phenol–chloroform extraction. *Anal Biochem* 1987;**162**:156-9.

[18] Sejima T, Madoiwa S, Mimuro J, Sugo T, Ishida T, Ichimura K, et al. Expression profiles of fibrinolytic components in nasal mucosa. *Histochem Cell Biol* 2004;**122**:61-73.

[19] Merskey C, Johnson AJ, Kleiner GJ, Wohl H. The defibrination syndrome: clinical features and laboratory diagnosis. *Br J Haematol* 1967;**13**:528-49.

[20] See WA, Yong X, Crist S, Hedican S. Diversity and modulation of plasminogen activator activity in human transitional carcinoma cell lines. *J Urol* 1994;**151**:1691-6.

[21] Horstman WG, McFarland RM, Gorman JD. Color Doppler sonographic findings in patients with transitional cell carcinoma of the bladder and renal pelvis. *J Ultrasound Med* 1995;**14**:129-33.
[22] Lapham RL, Ro JY, Staerkel GA, Ayala AG. Pathology of transitional cell carcinoma of the bladder and its clinical implications. *Sem Surg Oncol* 1997;**13**:307-18.
[23] Roberts KE, Hamele-Bena D, Saqi A, Stein CA, Cole RP. Pulmonary tumor embolism: a review of the literature. *Am J Med* 2003;**115**:228-32.
[24] Dail DH, Hammar SP. Pulmonary Pathology. 2nd ed. NewYork: Springer-Verlag; 1994.
[25] von Herbay A, Illes A, Waldherr R, Otto HF. Pulmonary tumor thrombotic microangiopathy with pulmonary hypertension. *Cancer* 1990;**66**:587-92.
[26] Arkel YS. Thrombosis and cancer. *Semin Oncol* 2000;**27**: 362-74.
[27] Kwaan HC, Gordon LI. Thrombotic microangiopathy in the cancer patient. *Acta Haematol* 2001;**106**:52-6.
[28] Tagnon HJ, Whitmore Jr WF, Shulman NR. Fibrinolysis in metastatic cancer of the prostate. *Cancer* 1952;**5**: 9-12.
[29] Gerke V, Moss SE. Annexins: from structure to function. *Physiol Rev* 2002;**82**:331-71.
[30] Deora AB, Kreitzer G, Jacovina AT, Hajjar KA. An annexin 2 phosphorylation switch mediates p11-dependent translocation of annexin 2 to the cell surface. *J Biol Chem* 2004;**279**:43411-8.
[31] Wright JF, Kurosky A, Wasi S. An endothelial cell-surface form of annexin II binds human cytomegalovirus. *Biochem Biophys Res Commun* 1994;**198**:983-9.
[32] Chung CY, Erickson HP. Cell surface annexin II is a high affinity receptor for the alternatively spliced segment of tenascin-C. *J Cell Biol* 1994;**126**:539-48.
[33] Hajjar KA, Guevara CA, Lev E, Dowling K, Chacko J. Interaction of the fibrinolytic receptor, annexin II, with the endothelial cell surface. Essential role of endonexin repeat 2. *J Biol Chem* 1996;**271**:21652-9.
[34] Hajjar KA, Menell JS. Annexin II: a novel mediator of cell surface plasmin generation. *Ann N Y Acad Sci* 1997;**811**: 337-49.
[35] Meddeb B, Guermazi S, Hafsia R, Ben Abid H, Gouider E, Ben Lakhal R, et al. Atypical defibrination syndromes and acute leukemias with a *t*(9,22) translocation, apropos of 2 cases. *Pathol Biol (Paris)* 2001;**49**:232-6.
[36] Olwill SA, McGlynn H, Gilmore WS, Alexander HD. Annexin II cell surface and mRNA expression in human acute myeloid leukaemia cell lines. *Thromb Res* 2005;**115**: 109-114.
[37] Plow EF, Freaney DE, Plescia J, Miles LA. The plasminogen system and cell surfaces: evidence for plasminogen and urokinase receptors on the same cell type. *J Cell Biol* 1986;**103**:2411-20.
[38] Kassam G, Choi KS, Ghuman J, Kang HM, Fitzpatrick SL, Zackson T, et al. The role of annexin II tetramer in the activation of plasminogen. *J Biol Chem* 1998;**273**:4790-9.
[39] Choi KS, Fogg DK, Yoon CS, Waisman DM. p11 regulates extracellular plasmin production and invasiveness of HT1080 fibrosarcoma cells. *FASEB J* 2003;**17**:235-46.
[40] Breast cancer progression working party. Evidence for novel non-angiogenic pathway in breast-cancer metastasis. *Lancet* 2000;**355**:1787-8.
[41] Shirakawa K, Tsuda H, Heike Y, Kato K, Asada R, Inomata M, et al. Absence of endothelial cells, central necrosis, and fibrosis are associated with aggressive inflammatory breast cancer. *Cancer Res* 2001;**61**:445-51.
[42] Hendrix MJ, Seftor EA, Meltzer PS, Gardner LM, Hess AR, Kirschmann DA, et al. Expression and functional significance of VE-cadherin in aggressive human melanoma cells: role in vasculogenic mimicry. *Proc Natl Acad Sci U S A* 2001;**98**:8018-23.
[43] Hendrix MJ, Seftor EA, Hess AR, Seftor RE. Vasculogenic mimicry and tumour-cell plasticity: lessons from melanoma. *Nat Rev Cancer* 2003;**3**:411-21.
[44] Ruf W, Seftor EA, Petrovan RJ, Weiss RM, Gruman LM, Margaryan NV, et al. Differential role of tissue factor pathway inhibitors 1 and 2 in melanoma vasculogenic mimicry. *Cancer Res* 2003;**63**:5381-9.
[45] Ling Q, Jacovina AT, Deora A, Febbraio M, Simantov R, Silverstein RL, et al. Annexin II regulates fibrin homeostasis and neoangiogenesis in vivo. *J Clin Invest* 2004; **113**:38-48.
[46] Semov A, Moreno MJ, Onichtchenko A, Abulrob A, Ball M, Ekiel I, et al. Metastasis-associated protein S100A4 induces angiogenesis through interaction with Annexin II and accelerated plasmin formation. *J Biol Chem* 2005;**280**: 20833-41.
[47] Hanford HA, Wong CA, Kassan H, Cundiff DL, Chandel N Underwood S, et al. Angiostatin(4.5)-mediated apoptosis of vascular endothelial cells. *Cancer Res* 2003;**63**: 4275-80.
[48] Wang H, Schultz R, Hong J, Cundiff DL, Jiang K, Soff GA. Cell surface-dependent generation of angiostatin4.5. *Cancer Res* 2004;**64**:162-8.

Arteriosclerosis, Thrombosis, and Vascular Biology

JOURNAL OF THE AMERICAN HEART ASSOCIATION

American Heart Association®

Learn and Live℠

Silencing of a Targeted Protein in In Vivo Platelets Using a Lentiviral Vector Delivering Short Hairpin RNA Sequence

Tsukasa Ohmori, Yuji Kashiwakura, Akira Ishiwata, Seiji Madoiwa, Jun Mimuro and Yoichi Sakata

Arterioscler. Thromb. Vasc. Biol. 2007;27;2266-2272; originally published online Sep 13, 2007;
DOI: 10.1161/ATVBAHA.107.149872
Arteriosclerosis, Thrombosis, and Vascular Biology is published by the American Heart Association. 7272 Greenville Avenue, Dallas, TX 72514
 Print ISSN: 1079-5642. Online ISSN: 1524-4636

Silencing of a Targeted Protein in In Vivo Platelets Using a Lentiviral Vector Delivering Short Hairpin RNA Sequence

Tsukasa Ohmori, Yuji Kashiwakura, Akira Ishiwata, Seiji Madoiwa, Jun Mimuro, Yoichi Sakata

Objective—Because platelets are anucleate cells having a limited life span, direct gene manipulation cannot in principle be used to investigate the involvement of a specific signal transduction pathway in platelet activation. In this study, we examined whether the expression of a short hairpin RNA (shRNA) sequence in hematopoietic stem cells is maintained during megakaryocyte differentiation, thus resulting in inhibition of targeted protein in platelets.

Methods and Results—To identify platelets derived from transduced stem cells, we generated a lentiviral vector that simultaneously expresses the shRNA sequence driven by the U6 promoter and GFP under the control of the glycoprotein (GP) Ibα promoter. Transplantation of mouse bone marrow cells transduced with the vector facilitated specifically mark platelets derived from the transduced cells. Transplantation of cells transduced with shRNA sequence targeting integrin αIIb caused a significant reduction of integrin αIIbβ3 (αIIbβ3) expression in GFP-positive platelets. It also inhibited αIIbβ3 activation assessed by the binding of JON/A, an antibody that recognizes activated αIIbβ3. Talin-1 silencing by the same method resulted in normal αIIbβ3 expression but deficient inside-out αIIbβ3 signaling.

Conclusions—shRNA expression driven by the U6 promoter is preserved during megakaryopoiesis. This method facilitates functional analysis of targeted protein in platelet activation. (***Arterioscler Thromb Vasc Biol.* 2007;27:2266-2272.**)

Key Words: shRNA ■ RNA interference ■ platelets ■ talin ■ integrin

Platelets are terminally-differentiated circulating anucleate cells whose adhesive and signaling functions are essential for normal hemostasis. Platelets are produced in the bone marrow from megakaryocytes as cytoplasmic fragments without genomic DNA.[1] Although platelets contain mRNA within their cytoplasm and can respond to physiological stimuli using biosynthetic processes regulated at the protein translation level,[2,3] application of direct genetic manipulation in platelets has not been reported. Alternatively, megakaryocyte lineage cells derived from embryonic or hematopoietic stem cells are amenable to genetic manipulation using gene transduction systems, enabling molecular studies of adhesion and signaling in megakaryocytes in a way not possible with platelets.[4,5]

Because platelets and their precursor megakaryocytes have a finite lifespan, hematopoietic stem cells are preferable targets for genetic transfer to establish long-term in vivo expression of the targeted protein in platelets.[6] When a retroviral vector containing the integrin β3 (β3) gene driven by the integrin αIIb (αIIb) promoter was transduced into $CD34^+$ cells from a Glanzmann thrombasthenia patient with defects in the β3 gene, integrin αIIbβ3 (αIIbβ3) was detected after in vitro megakaryocyte differentiation.[7] We have previously shown that transduction of hematopoietic stem cells with lentiviral vector harboring the glycoprotein (GP) Ibα promoter enables specific and efficient expression of the targeted protein in platelets in vivo.[8] Further, the therapeutic expression of αIIbβ3 in β3-deficient mice using a lentivirus vector containing β3 complimentary DNA (cDNA) under the control of the αIIb promoter has been reported.[9] These data indicate that gene expression driven by a platelet-specific promoter using the transduction of hematopoietic stem cells with lentiviral vector can be applied to investigations of the involvement of specific proteins in platelet signaling pathways. However, there has been no evaluation of whether the knock-down of targeted proteins in hematopoietic stem cells using a short hairpin RNA (shRNA) sequence results in sufficient protein reduction in platelets. In this study, we examined whether shRNA expression driven by the RNA polymerase III promoter is sustained during megakaryopoiesis, and whether gene silencing with shRNAs is applicable to analyzing the functions of αIIbβ3 in in vivo platelets.

Materials and Methods

Materials, cDNA cloning, transfection, construction of lentiviral vector, stem cell transplantation, flow cytometry, immunoblotting, RT–polymerase chain reaction (PCR), platelet adhesion assay, and

Original received March 26, 2007; final version accepted July 19, 2007.

From the Research Division of Cell and Molecular Medicine, Center for Molecular Medicine, Jichi Medical University School of Medicine, Tochigi, Japan.

Correspondence to Tsukasa Ohmori, MD, PhD or Yoichi Sakata, MD, PhD, Research Division of Cell and Molecular Medicine, Center for Molecular Medicine, Jichi Medical University School of Medicine, 3111-1 Yakushiji, Shimotsuke, Tochigi 329-0498, Japan. E-mail tohmori@jichi.ac.jp or yoisaka@jichi.ac.jp.

Arterioscler Thromb Vasc Biol. is available at http://atvb.ahajournals.org

DOI: 10.1161/ATVBAHA.107.149872

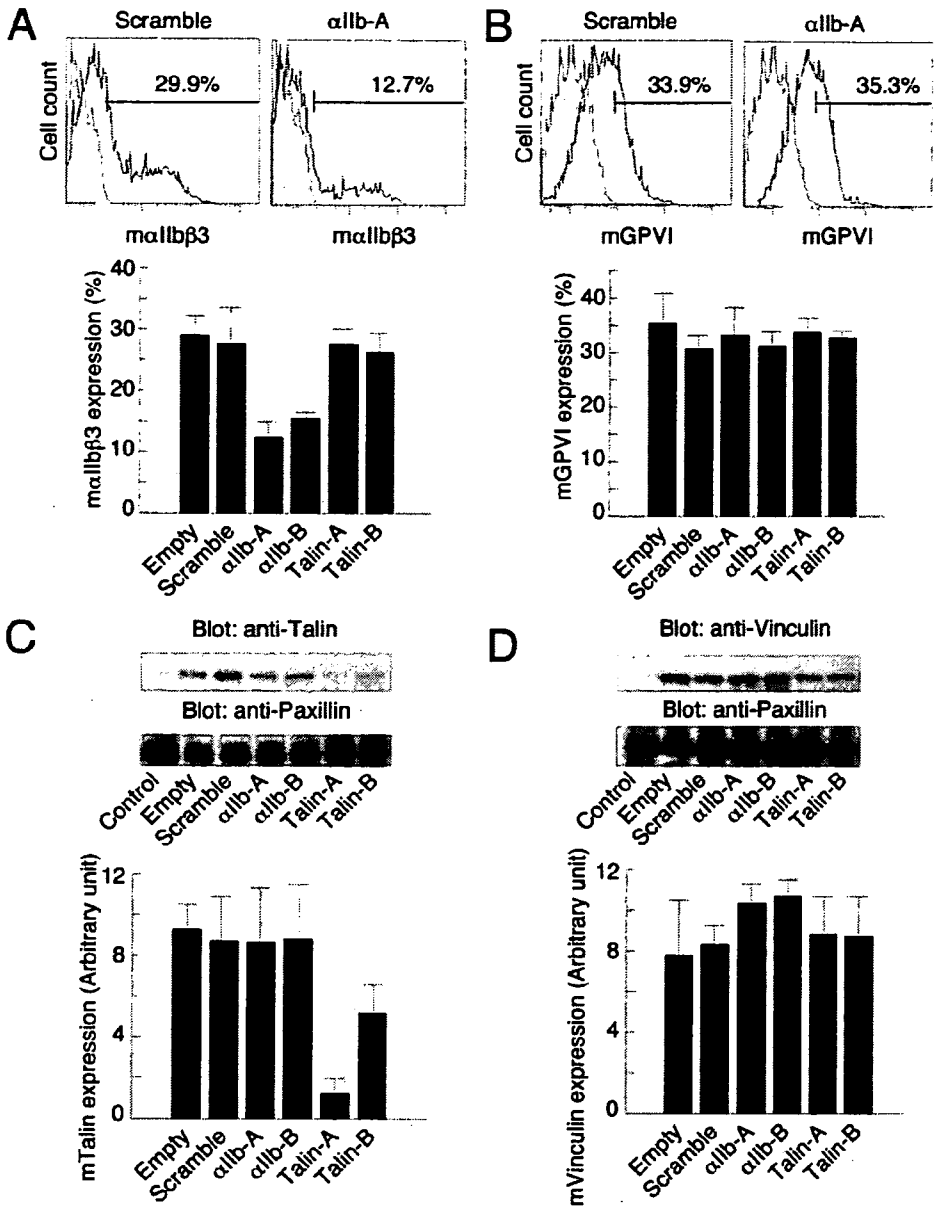

Figure 1. Inhibition of ectopic expression of the target protein by a lentiviral vector construct delivering shRNA in HEK293 cells. HEK293 cells were cotransfected with expression plasmid containing cDNA of mouse integrin αIIb and integrin β3 (A), GPVI (B), Talin (C), or vinculin (D) and the lentiviral siRNA vector plasmid containing no RNA sequence (Empty), scramble RNA sequence (Scramble), αIIbA sequence (αIIb-A), αIIbB sequence (αIIb-B), talinA sequence (Talin-A), or talinB sequence (Talin-B). After 48 hours, protein expressions were examined by flow cytometry or immunoblotting. The data are representative of 3 experiments. In lower panel, protein expression after transfection was quantified. Columns and error bars represent the mean±SD (n=3 per group).

immunohistochemistry are described in detail in the supplemental materials, available online at http://atvb.ahajournals.org.

Results

Efficient GFP Expression in Platelets Using LentiLox Vector Harboring *GPIbα* Promoter In Vivo

We first substituted the CMV promoter of pLL3.7, a lentiviral gene transfer vector which simultaneously expresses shRNA and GFP (LentiLox-CMV),[10] with the platelet-specific GPIbα promoter (LentiLox-GPIbα) (supplemental Figure I). To compare strengths and the specificities of the CMV and GPIbα promoters and to assess GFP transduction using these lentiviral vectors in vivo, bone marrow cells transduced with LentiLox-CMV or LentiLox-GPIbα were transplanted into the recipient mice. When bone marrow cells transduced with LentiLox-CMV were transplanted, GFP expression was observed in 14% to 32% of $CD45^+$ cells and in 0.7 to 2.4% of platelets in peripheral blood (supplemental Figure II). As described previously,[8] transduction with LentiLox-GPIbα resulted in efficient GFP gene marking in platelets (10% to 22%); however, only marginal GFP expression was observed in $CD45^+$ and red blood cells (supplemental Figure II). These data suggested that the LentiLox-GPIbα

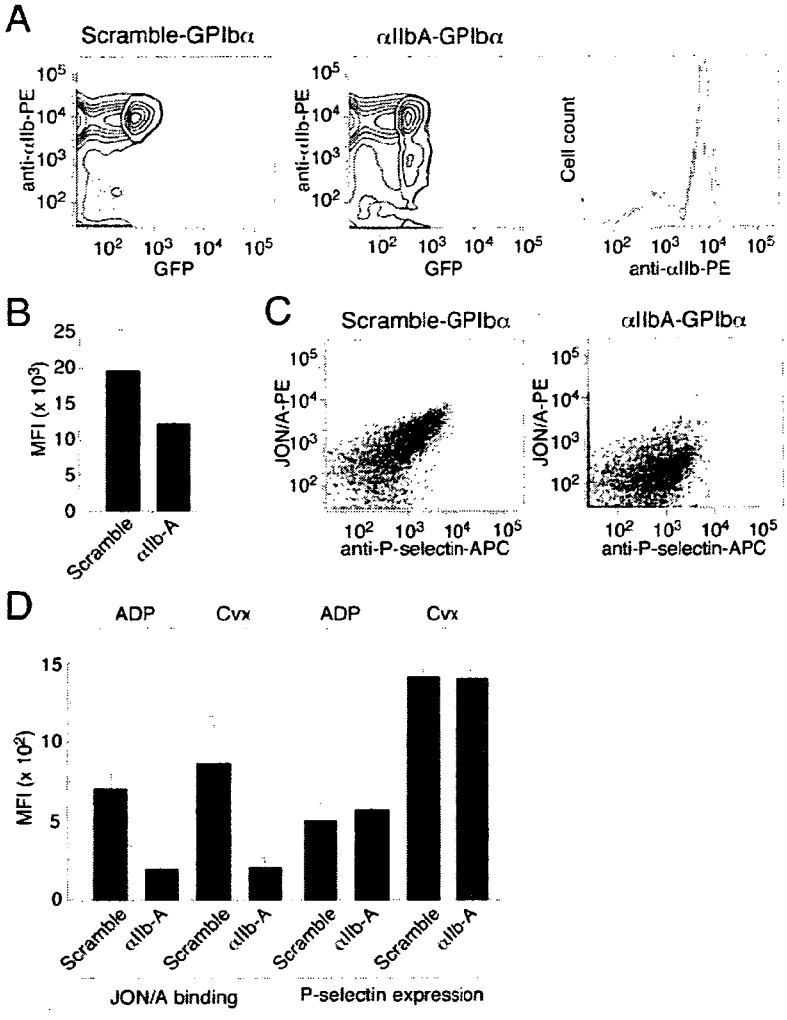

Figure 2. Silencing of endogenous integrin $\alpha IIb\beta 3$ in platelets. Bone marrow cells from donor mice were transduced with LentiLox-scramble-GPIbα or LentiLox-αIIbA-GPIbα at an MOI of 30. Each irradiated recipient mouse received 2 000 000 transduced cells. A, Representative flow cytometry analyses of integrin $\alpha IIb\beta 3$ expression in platelets of peripheral blood are shown 30 days after transplantation. The plots represent the degree of GFP expression (horizontal) and specific antibody binding for integrin αIIb (vertical). The specific antibody binding in GFP-positive platelets is shown (right panel; white:Lentilox-scramble-GPIbα, gray: LentiLox-αIIbA-GPIbα). B, Columns and error bars represent the mean±SD of mean fluorescence intensity of antibody binding for αIIb in GFP-positive platelets (n=9 per group). C, The activation of $\alpha IIb\beta 3$ assessed by JON/A binding and P-selectin expression in platelets stimulated with 150 ng/mL of convulxin. The plots represent the degree of P-selectin expression (horizontal) and JON/A binding (vertical) in GFP-positive platelets. D, Columns and error bars represent the mean±SD of mean fluorescence intensity (MFI) of antibody binding after stimulation with 6 μmol/L ADP or 150 ng/mL of convulxin to GFP-positive platelets (n=5 to 7 per group).

system enables specific GFP marking of platelets derived from transduced hematopoietic stem cells.

Efficiency of Lentiviral shRNA for Silencing of Targeted Protein Expression

We next validated the effects of shRNA sequence expression driven by the U6 promoter in LentiLox on expression of the targeted protein. We selected the shRNA sequences for integrin αIIb (supplemental Figure IB), so that it was easy to validate the expression and function of this protein using flow cytometry. We also chose talin-1 sequences as a test case for intracellular protein (supplemental Figure IB); because talin is responsible for β integrin activation but its function in in vivo platelets has not been evaluated. Because a molecular defect affecting 1 of the 2 integrin-coding genes is sufficient to cause a concomitant deficit of both αIIb and $\beta 3$,[11] we prepared the 2 expression plasmids containing cDNA of αIIb and $\beta 3$ for the expression of $\alpha IIb\beta 3$ complexes. To determine the efficiency of lentiviral shRNA for αIIb-A, the surface expression of $\alpha IIb\beta 3$ in HEK293 cells was determined after cotransfection of the shRNA constructs with integrin αIIb and $\beta 3$ expression plasmids. As shown in Figure 1A, $\alpha IIb\beta 3$ expression on the cell surface was significantly inhibited by cotransfection with the shRNA constructs for αIIb. On the other hand, other shRNA sequences did not affect the surface expression of $\alpha IIb\beta 3$ (Figure 1A). As well, shRNA sequences for talin-1 specifically inhibited ectopically-expressed talin in HEK293 cells (Figure 1C). Sequences for αIIb-A and talin did not influence the expressions of GPVI and vinculin (Figure 1B and 1D). The degradation of mRNA by shRNA expression was confirmed by real-time quantitative RT-PCR (supplemental Figure III). The construct expressing the shRNA sequence αIIb-A and talin-A caused a more powerful inhibition of the expressions of αIIb and talin, respectively (Figure 1A and 1C). To rule out the off-targeting effect caused by the high concentration of shRNA, we validated the specificity of these shRNA sequences by a lower concentration of plasmid vectors (0.2 μg; data not shown). Hence, we selected the αIIbA and talin-A sequences for in vivo experiments.

Silencing of $\alpha IIb\beta 3$ Expression In Vivo Platelets by Transplantation of Transduced Bone Marrow Cells With shRNA Lentiviral Vector

We next examined the effects of shRNA driven by the U6 promoter during megakaryopoiesis in vivo. The bone marrow cells transduced with LentiLox-GPIb containing the scramble

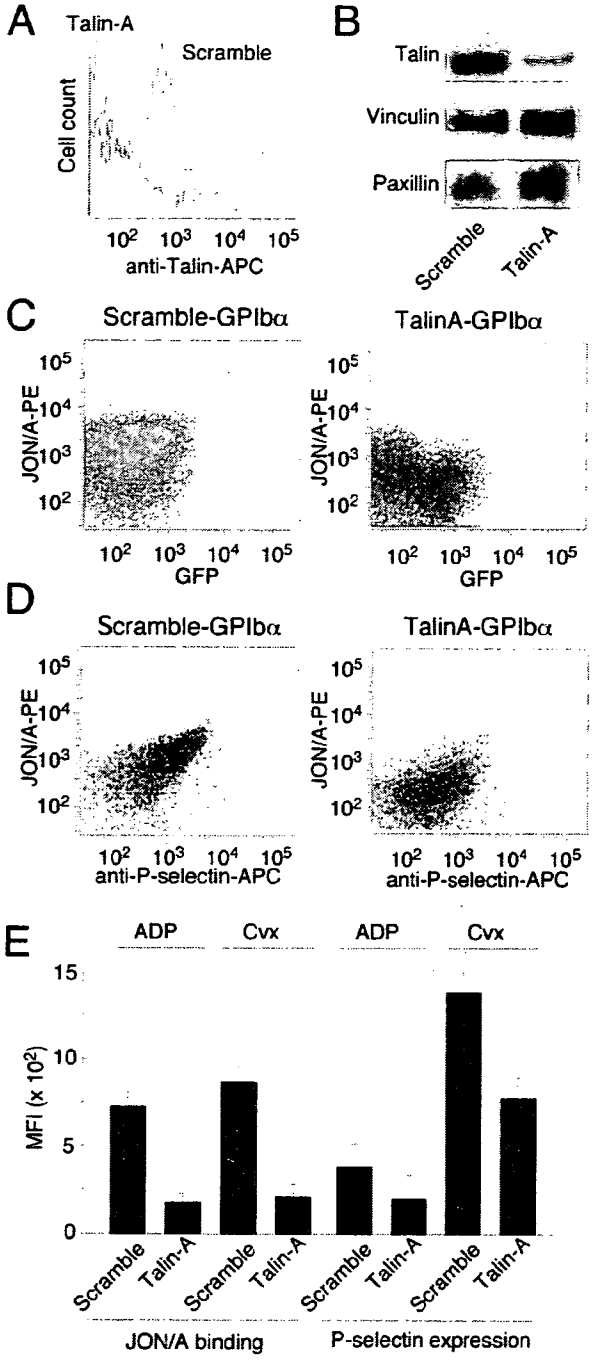

Figure 3. Knockdown of talin-1 inhibits integrin αIIbβ3 activation and P-selectin expression in platelets. Bone marrow cells transfected with LentiLox-scramble-GPIbα or LentiLox-talinA-GPIbα were transplanted into recipient mice. A, Representative flowcytometry analyses of intracellular talin expression in GFP-positive (white: LentiLox-scramble-GPIbα; gray: Lentilox-talinA-GPIbα). B, After the sorting of GFP-positive platelets, the platelet lysates were immunoblotted with anti-talin MoAb (upper panel), anti-vinculin polyclonal antibody (middle panel), or anti-paxillin antibody (lower panel). C, Activation of αIIbβ3 was assessed by JON/A binding to platelets incubated with 150 ng/mL of convulxin. The plots represent the degree of GFP expression (horizontal) and specific antibody binding (vertical). D, Activation of αIIbβ3 assessed by JON/A binding and P-selectin expression in GFP-positive platelets stimulated with 150 ng/mL of convulxin. The plots represent the degree of P-selectin expression (horizontal) and JON/A binding (vertical). E, Columns and error bars represent the mean±SD of mean fluorescence intensity (MFI) of antibody binding after stimulation with 6 μmol/L ADP or 150 ng/mL of convulxin to GFP-positive platelets (n=7 to 11 per group).

sequence (LentiLox-scramble-GPIbα) or αIIbA sequence (LentiLox-αIIbA-GPIbα) were transplanted into recipient mice. After transplantation, GFP expression was observed in 15% to 20% of platelets in both transplanted groups (data not shown). It is of note that αIIbβ3 expression in GFP-positive platelets was significantly reduced in the recipient mice transplanted with cells transduced with LentiLox-αIIbA-GPIbα (Figure 2A and 2B). As well, JON/A binding after ADP stimulation, which recognizes activated αIIbβ3, was reduced to a greater extent by the transduction with LentiLox-αIIbA-GPIbα (Figure 2B and 2D). The discrepancy in the results between αIIbβ3 expression and JON/A binding is thought to be partly the result of the expression of an incompetent αIIbβ3 complex that is recognized as antigen but does not act as functional receptor. Because αIIb is the most abundant protein in platelets, it is possible that mRNA degradation of αIIb by siRNA in platelets becomes incomplete. Under the same conditions, GPIb and GPVI expressions were not affected (data not shown). Additionally, P-selectin expression after platelet activation was hardly affected (Figure 2C and 2D). These data suggested that the expression of the shRNA sequence driven by the U6 promoter is maintained during megakaryopoiesis, and that this method can be applied to investigations of the involvement of specific proteins in platelet activation.

Silencing of Talin in Platelets Decreases αIIbβ3 Activation

We next examined whether talin-1 knockdown affects αIIbβ3 activation in in vivo platelets, using shRNA silencing. Although talin is believed to be involved in the final common step of integrin αIIbβ3 activation,[12] functional analysis in in vivo platelets has not been performed. When bone marrow cells transduced with LentiLox-scramble-GPIbα or LentiLox-talinA-GPIbα at an MOI of 30 were transplanted, we confirmed the inhibition of talin expression in platelets derived from the cells transduced with LentiLox-talinA-GPIbα by intracellular flowcytometry (Figure 3A). In addition, talin reduction was also verified after sorting of GFP-positive platelets by immunoblotting (Figure 3B). On the other hand, the expressions of αIIbβ3, GPIbα, and GPVI were not affected (data not shown). As shown in Figure 3C through 3E, in talin-deficient platelets identified as GFP-positive cells, αIIbβ3 activation after ADP or convulxin stimulation was significantly decreased. Furthermore, talin-deficient platelet partly affected the expression of P-selectin after the platelet stimulation (Figure 3D and 3E). These data clarified that talin was involved not only in αIIbβ3-dependent platelet activation but also in the release reaction in actual platelets.

Finally, using a platelet adhesion assay we attempted to determine whether talin-deficient platelets influenced the spreading onto fibrinogen. Platelet adhesion to immobilized

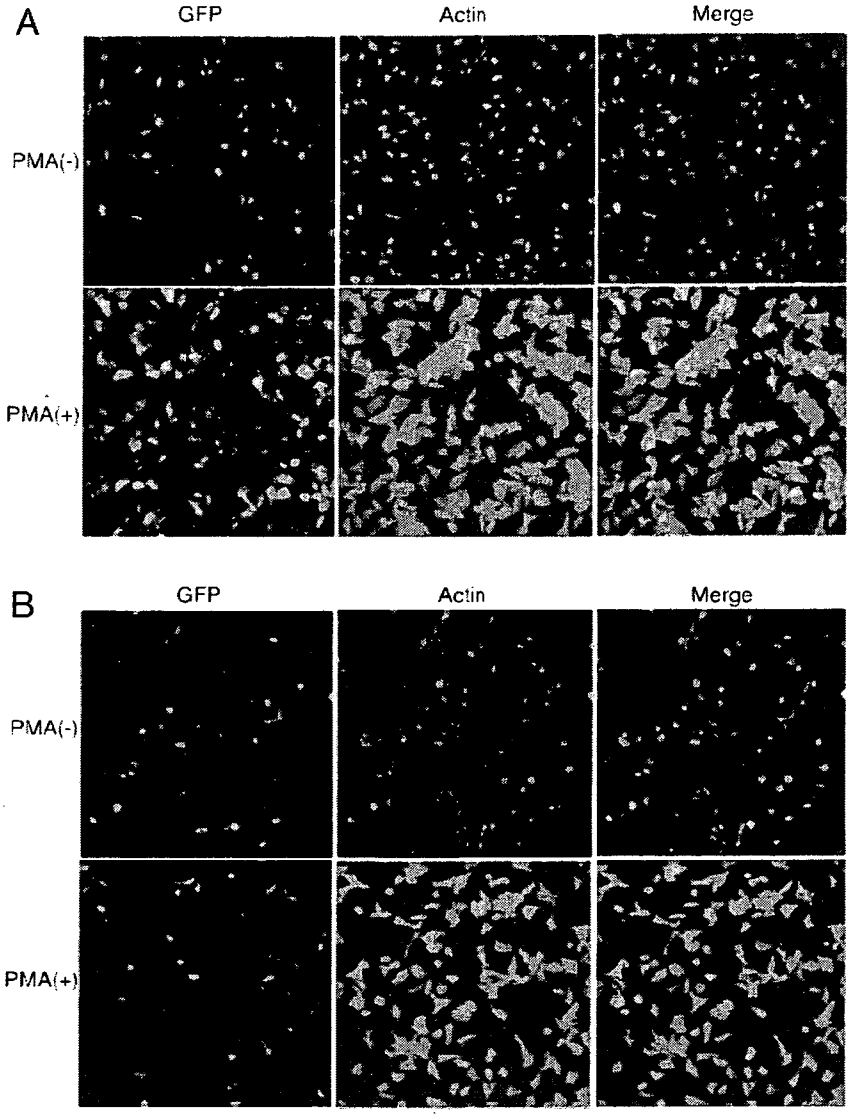

Figure 4. Failure of talin-deficient platelets to spread onto immobilized fibirinogen after stimulation with PMA. Bone marrow cells transfected with LentiLox-scramble-GPIbα (A) or LentiLox-talinA-GPIbα (B) were transplanted into recipient mice. Washed platelets treated without (upper panel) or with 1 μmol/L PMA (lower panel) were placed on immobilized fibrinogen for 30 minutes. Cells were fixed and then stained with anti-GFP antibody (green; left panel) and rhodamine-conjugated phalloidin (red; middle panel), as described in Materials and Methods. The merged images show colocalization of GFP and actin staining (yellow; right panel). The data are representative of 3 independent experiments.

fibrinogen by itself was not inhibited by the deficiency of talin (Figure 4). However, platelet spreading after stimulation with PMA was markedly suppressed (Figure 4), suggesting that talin is required for platelet spreading on fibrinogen.

Discussion

RNA interference using siRNAs to inhibit specific gene expression is a powerful and promising technology for both basic research and therapeutic intervention.[13,14] A number of vector systems have been reported to mediate stable transduction and expression of shRNAs in mammalian cells.[13] Among them, lentiviral vectors have been demonstrated to have the ability to stably transduce nondividing cells such as stem cells through integration of the vector DNA into the genome.[10,15] RNA polymerase III promoters, most commonly the H1 and U6 promoters, have been incorporated into the lentiviral vectors for stable expression of shRNAs.[13] The potential problem for functional genomics studies inherent in transfection with shRNA is variability in transfection efficiency. A solution to this problem is coexpression of reporter genes such as GFP, which facilitates the selection of transduced cells. To obtain efficient gene marking of platelets derived from transduced hematopoietic stem cells, we substituted the ubiquitous CMV promoter of LentiLox with the platelet-specific GPIbα promoter and showed that transplantation of bone marrow cells transduced with the vector enabled specific marking of platelets derived from transduced hematopoietic stem cells expressing shRNA sequence.

Platelets are terminally-differentiated anucleate cells, and for this reason direct gene transfer and silencing using virus or plasmid vector have been thought to be impossible. Since the development of gene targeting technologies in embryonic stem cells,[16] the "gold standard" for the analysis of gene function in platelets has been the creation of knockout mice. A large number of knockout studies have shown aberrant platelet phenotypes.[17–20] However, one of the major drawbacks of conventional knockouts is that if the gene product is essential in many tissues, then it is quite likely that the consequence of homozygosity for the mutated allele will be lethality. Several experimental strategies are used or have the

potential to overcome the problem of lethality. First, improvements in the technological procedures have allowed for refined analyses of gene functions at specific developmental stages or in specific tissues, based on conditional knock-out strategies by means of Cre-lox–regulated recombination.[21] Another solution, which has been applied in a few cases, is to use hematopoietic cells from fetal liver of knockout embryos to reconstitute the hematopoietic system of lethally-irradiated wild-type animals.[22,23] Despite these significant improvements, the creation of loss-of-function alleles in the mouse remains time-consuming and costly. Our demonstration that the expression of shRNAs driven by RNA polymerase III promoters can be used to functionally silence protein expression in platelets suggests that RNAi-based technologies might represent a convenient strategy for the study of platelet signal transduction. Our methods could in fact detect platelets derived from transduced stem cells as GFP-positive platelets, and so enable the examination of the involvement of target proteins in platelet signal transduction by flow cytometry and adhesion assay. However, GFP-positive platelets after the transplantation were limited by up to 20% in our protocols. Hence, platelet aggregation testing and the analysis of intracellular signaling pathways including tyrosine phosphorylation are not thought impossible. Higher transfection efficiencies would be required to demonstrate genuine effects and to be a valid alternative to making gene knockout mice.

Cellular control of integrin activation is essential for normal development because it controls cell adhesion, migration, and assembly of the extracellular matrix.[24,25] Platelets express members of the $\beta 1$ subfamily ($\alpha v\beta 1$, $\alpha 2\beta 1$, and $\alpha 6\beta 1$) that support platelet adhesion to the extracellular matrix proteins including collagen and laminins, as well as expressing members of the $\beta 3$ subfamily ($\alpha v\beta 3$ and $\alpha IIb\beta 3$).[24] Among them, $\alpha IIb\beta 3$, a receptor for fibrinogen, von Willebrand factor (VWF), fibronectin, and vitronectin is an essential requirement for platelet aggregation. Integrin activation can be controlled by signaling pathways that are thought to act by regulating specific interactions between cytoplasmic proteins and the integrin—or β-subunit—cytoplasmic tail.[25,26] Although many types of proteins interacting with integrin cytoplasmic tails have been reported to be involved in platelet aggregation,[12,27–31] functional analysis of in vivo platelets has not been reported; embryos lacking these proteins, including talin, vinculin, FAK, and Cas do not normally grow in the uterus.[32–35] Talin is a major cytoskeletal protein that colocalizes with activated integrins and binds to integrin β cytoplasmic domains; with the overexpression of the N-terminal region of talin results in activation of integrins.[14,28,36] Additionally, binding of talin to integrin β tails has been shown to be a common final step in integrin activation.[12] In this study, using a method involving RNA interference, we clearly demonstrated that talin is involved in $\alpha IIb\beta 3$-dependent platelet activation in in vivo platelets. Furthermore, talin might partly participate in the α-granule release reaction. These results confirmed that this strategy could be useful as a convenient and powerful method to investigate the role of specific proteins in platelet activation in vivo.

Acknowledgments

We thank N. Matsumoto and M. Ito for their excellent technical assistance.

Sources of Funding

This work was supported by Grants from the Mitsubishi Pharma Research Foundation; Grants-in-aid for Scientific Research from the Ministry of Education and Science; Health and Labor Science Research Grants for Research from Ministry of Health, Labor, and Welfare; and Grants for "High-Tech Center Research" Projects for Private Universities: matching fund subsidy from MEXT (Ministry of Education, Culture, Sports, Science, and Technology), 2002–2006.

Disclosures

None.

References

1. Italiano JE Jr, Shivdasani RA. Megakaryocytes and beyond: the birth of platelets. *J Thromb Haemost.* 2003;1:1174–1182.
2. Brogren H, Karlsson L, Andersson M, Wang L, Erlinge D, Jern S. Platelets synthesize large amounts of active plasminogen activator inhibitor 1. *Blood.* 2004;104:3943–3948.
3. Maguire PB, Fitzgerald DJ. Platelet proteomics. *J Thromb Haemost.* 2003;1:1593–1601.
4. Eto K, Murphy R, Kerrigan SW, Bertoni A, Stuhlmann H, Nakano T, Leavitt AD, Shattil SJ. Megakaryocytes derived from embryonic stem cells implicate CalDAG-GEFI in integrin signaling. *Proc Natl Acad Sci U S A.* 2002;99:12819–12824.
5. Shiraga M, Ritchie A, Aidoudi S, Baron V, Wilcox D, White G, Ybarrondo B, Murphy G, Leavitt A, Shattil S. Primary megakaryocytes reveal a role for transcription factor NF-E2 in integrin alpha IIb beta 3 signaling. *J Cell Biol.* 1999;147:1419–1430.
6. Wilcox DA, White GC 2nd. Gene therapy for platelet disorders: studies with Glanzmann's thrombasthenia. *J Thromb Haemost.* 2003;1:2300–2311.
7. Wilcox DA, Olsen JC, Ishizawa L, Bray PF, French DL, Steeber DA, Bell WR, Griffith M, White GC 2nd. Megakaryocyte-targeted synthesis of the integrin beta(3)-subunit results in the phenotypic correction of Glanzmann thrombasthenia. *Blood.* 2000;95:3645–3651.
8. Ohmori T, Mimuro J, Takano K, Madoiwa S, Kashiwakura Y, Ishiwata A, Niimura M, Mitomo K, Tabata T, Hasegawa M, Ozawa K, Sakata Y. Efficient expression of a transgene in platelets using simian immunodeficiency virus-based vector harboring glycoprotein Ibalpha promoter: in vivo model for platelet-targeting gene therapy. *Faseb J.* 2006;20:1522–1524.
9. Fang J, Hodivala-Dilke K, Johnson BD, Du LM, Hynes RO, White GC 2nd, Wilcox DA. Therapeutic expression of the platelet-specific integrin, alphaIIbbeta3, in a murine model for Glanzmann thrombasthenia. *Blood.* 2005;106:2671–2679.
10. Rubinson DA, Dillon CP, Kwiatkowski AV, Sievers C, Yang L, Kopinja J, Rooney DL, Ihrig MM, McManus MT, Gertler FB, Scott ML, Van Parijs L. A lentivirus-based system to functionally silence genes in primary mammalian cells, stem cells and transgenic mice by RNA interference. *Nat Genet.* 2003;33:401–406.
11. Perutelli P, Mori PG. Biochemical and molecular basis of Glanzmann's thrombasthenia. *Haematologica.* 1992;77:421–426.
12. Tadokoro S, Shattil SJ, Eto K, Tai V, Liddington RC, de Pereda JM, Ginsberg MH, Calderwood DA. Talin binding to integrin beta tails: a final common step in integrin activation. *Science.* 2003;302:103–106.
13. Amarzguioui M, Rossi JJ, Kim D. Approaches for chemically synthesized siRNA and vector-mediated RNAi. *FEBS Lett.* 2005;579:5974–5981.
14. Li CX, Parker A, Menocal E, Xiang S, Borodyansky L, Fruehauf JH. Delivery of RNA interference. *Cell Cycle.* 2006;5:2103–2109.
15. Woods NB, Ooka A, Karlsson S. Development of gene therapy for hematopoietic stem cells using lentiviral vectors. *Leukemia.* 2002;16:563–569.
16. Thomas KR, Capecchi MR. Site-directed mutagenesis by gene targeting in mouse embryo-derived stem cells. *Cell.* 1987;51:503–512.
17. Clements JL, Lee JR, Gross B, Yang B, Olson JD, Sandra A, Watson SP, Lentz SR, Koretzky GA. Fetal hemorrhage and platelet dysfunction in SLP-76-deficient mice. *J Clin Invest.* 1999;103:19–25.

18. Pasquet JM, Gross B, Quek L, Asazuma N, Zhang W, Sommers CL, Schweighoffer E, Tybulewicz V, Judd B, Lee JR, Koretzky G, Love PE, Samelson LE, Watson SP. LAT is required for tyrosine phosphorylation of phospholipase cgamma2 and platelet activation by the collagen receptor GPVI. *Mol Cell Biol.* 1999;19:8326–8334.
19. Watson SP, Gibbins J. Collagen receptor signalling in platelets: extending the role of the ITAM. *Immunol Today.* 1998;19:260–264.
20. Offermanns S. Activation of platelet function through G protein-coupled receptors. *Circ Res.* 2006;99:1293–1304.
21. Tiedt R, Schomber T, Hao-Shen H, Skoda RC. Pf4-Cre transgenic mice allow generating lineage-restricted gene knockouts for studying megakaryocyte and platelet function in vivo. *Blood.* 2006.
22. Obergfell A, Eto K, Mocsai A, Buensuceso C, Moores SL, Brugge JS, Lowell CA, Shattil SJ. Coordinate interactions of Csk, Src, and Syk kinases with αIIbβ3 initiate integrin signaling to the cytoskeleton. *J Cell Biol.* 2002;157:265–275.
23. Matloubian M, Lo CG, Cinamon G, Lesneski MJ, Xu Y, Brinkmann V, Allende ML, Proia RL, Cyster JG. Lymphocyte egress from thymus and peripheral lymphoid organs is dependent on S1P receptor 1. *Nature.* 2004;427:355–360.
24. Bennett JS. Structure and function of the platelet integrin alphaIIbbeta3. *J Clin Invest.* 2005;115:3363–3369.
25. Zamir E, Geiger B. Molecular complexity and dynamics of cell-matrix adhesions. *J Cell Sci.* 2001;114:3583–3590.
26. Lo SH. Focal adhesions: what's new inside. *Dev Biol.* 2006;294:280–291.
27. Asijee GM, Sturk A, Bruin T, Wilkinson JM, Ten Cate JW. Vinculin is a permanent component of the membrane skeleton and is incorporated into the (re)organising cytoskeleton upon platelet activation. *Eur J Biochem.* 1990;189:131–136.
28. Calderwood DA, Zent R, Grant R, Rees DJ, Hynes RO, Ginsberg MH. The Talin head domain binds to integrin beta subunit cytoplasmic tails and regulates integrin activation. *J Biol Chem.* 1999;274:28071–28074.
29. Lipfert L, Haimovich B, Schaller MD, Cobb BS, Parsons JT, Brugge JS. Integrin-dependent phosphorylation and activation of the protein tyrosine kinase pp125FAK in platelets. *J Cell Biol.* 1992;119:905–912.
30. Ohmori T, Yatomi Y, Asazuma N, Satoh K, Ozaki Y. Involvement of proline-rich tyrosine kinase 2 in platelet activation: tyrosine phosphorylation mostly dependent on alphaIIbbeta3 integrin and protein kinase C, translocation to the cytoskeleton and association with Shc through Grb2. *Biochem J.* 2000;347:561–569.
31. Ohmori T, Yatomi Y, Inoue K, Satoh K, Ozaki Y. Tyrosine dephosphorylation, but not phosphorylation, of p130Cas is dependent on integrin alpha IIb beta 3-mediated aggregation in platelets: implication of p130Cas involvement in pathways unrelated to cytoskeletal reorganization. *Biochemistry.* 2000;39:5797–5807.
32. Honda H, Oda H, Nakamoto T, Honda Z, Sakai R, Suzuki T, Saito T, Nakamura K, Nakao K, Ishikawa T, Katsuki M, Yazaki Y, Hirai H. Cardiovascular anomaly, impaired actin bundling and resistance to Src-induced transformation in mice lacking p130Cas. *Nat Genet.* 1998;19:361–365.
33. Ilic D, Furuta Y, Kanazawa S, Takeda N, Sobue K, Nakatsuji N, Nomura S, Fujimoto J, Okada M, Yamamoto T. Reduced cell motility and enhanced focal adhesion contact formation in cells from FAK-deficient mice. *Nature.* 1995;377:539–544.
34. Monkley SJ, Zhou XH, Kinston SJ, Giblett SM, Hemmings L, Priddle H, Brown JE, Pritchard CA, Critchley DR, Fassler R. Disruption of the talin gene arrests mouse development at the gastrulation stage. *Dev Dyn.* 2000;219:560–574.
35. Xu W, Baribault H, Adamson ED. Vinculin knockout results in heart and brain defects during embryonic development. *Development.* 1998;125:327–337.
36. Calderwood DA. Talin controls integrin activation. *Biochem Soc Trans.* 2004;32:434–437.

Hypertension

Journal of the American Heart Association

American Heart Association®

Learn and Live℠

Adenoassociated Virus Mediated Prostacyclin Synthase Expression Prevents Pulmonary Arterial Hypertension in Rats

Takayuki Ito, Takashi Okada, Jun Mimuro, Hiroshi Miyashita, Ryosuke Uchibori, Masashi Urabe, Hiroaki Mizukami, Akihiro Kume, Masafumi Takahashi, Uichi Ikeda, Yoichi Sakata, Kazuyuki Shimada and Keiya Ozawa

Hypertension 2007;50;531-536; originally published online Jul 16, 2007;
DOI: 10.1161/HYPERTENSIONAHA.107.091348
Hypertension is published by the American Heart Association. 7272 Greenville Avenue, Dallas, TX 72514
 Print ISSN: 0194-911X. Online ISSN: 1524-4563

Adenoassociated Virus–Mediated Prostacyclin Synthase Expression Prevents Pulmonary Arterial Hypertension in Rats

Takayuki Ito, Takashi Okada, Jun Mimuro, Hiroshi Miyashita, Ryosuke Uchibori, Masashi Urabe, Hiroaki Mizukami, Akihiro Kume, Masafumi Takahashi, Uichi Ikeda, Yoichi Sakata, Kazuyuki Shimada, Keiya Ozawa

Abstract—Prostacyclin synthase (PGIS) is the final committed enzyme in the metabolic pathway of prostacyclin production. The therapeutic option of intravenous prostacyclin infusion in patients with pulmonary arterial hypertension is limited by the short half-life of the drug and life-threatening catheter-related complications. To develop a better delivery system for prostacyclin, we examined the feasibility of intramuscular injection of an adenoassociated virus (AAV) vector expressing PGIS for preventing monocrotaline-induced pulmonary arterial hypertension in rats. We developed an AAV serotype 1–based vector carrying a human PGIS gene (AAV-PGIS). AAV-PGIS or the control AAV vector expressing enhanced green fluorescent protein was injected into the anterior tibial muscles of 3-week–old male Wistar rats; this was followed by the monocrotaline administration at 7 weeks. Eight weeks after injecting the vector, the plasma levels of 6-keto-prostaglandin $F_{1\alpha}$ increased in a vector dose-dependent manner. At this time point, the PGIS transduction (1×10^{10} genome copies per body) significantly decreased mean pulmonary arterial pressure (33.9 ± 2.4 versus 46.1 ± 3.0 mm Hg; $P<0.05$), pulmonary vascular resistance (0.26 ± 0.03 versus 0.41 ± 0.03 mm Hg $\cdot$ mL^{-1} $\cdot$ min^{-1} $\cdot$ kg^{-1}; $P<0.05$), and medial thickness of the peripheral pulmonary artery ($14.6\pm1.5\%$ versus $23.5\pm0.5\%$; $P<0.01$) as compared with the controls. Furthermore, the PGIS-transduced rats demonstrated significantly improved survival rates as compared with the controls (100% versus 50%; $P<0.05$) at 8 weeks postmonocrotaline administration. An intramuscular injection of AAV-PGIS prevents monocrotaline-pulmonary arterial hypertension in rats and provides a new therapeutic alternative for preventing pulmonary arterial hypertension in humans. (***Hypertension.*** **2007;50:531-536.)**

Key Words: hypertension ■ pulmonary ■ gene therapy ■ remodeling ■ prostacyclin synthase

Pulmonary arterial hypertension (PAH) is an intractable disease that leads to increased pulmonary arterial pressure, progressive right heart failure, and premature death; however, no satisfactory treatment has been established for PAH.[1] Although intravenous prostacyclin (PGI_2) therapy prolongs survival in patients with PAH, the use of this treatment option is limited by the short half-life of the drug, requirement for a continuous infusion system, and catheter-related complications.[1,2] PGI_2 synthase (PGIS) is the final committed enzyme in the metabolic pathway of PGI_2 production. PGIS gene transfer is a promising approach for the stable production of endogenous PGI_2.[3–6] However, previous strategies have several limitations both in the selection of delivery routes and in the efficiency of gene expression. For instance, intratracheal gene transfer may deteriorate respiratory function in critically ill subjects, and the intrahepatic approach may cause peritonitis as a result of direct liver puncture. Although an intramuscular approach seems to be safer than the previous approaches, the conventional plasmid-based strategies achieved only transient gene expression and required repeated gene transfer to inhibit pathological remodeling of the pulmonary artery (PA).[6]

In this study, we used an adenoassociated virus (AAV) vector together with an intramuscular approach to obtain more efficient PGI_2 expression. AAV vectors permit efficient and sustained gene expression in nondividing skeletal muscle cells with minimal inflammatory and immune responses. We reported previously that a stable serum concentration of a secretory protein was achieved over a 1-year period by using a single intramuscular injection of several AAV vector (AAV2 and AAV5) serotypes in mice.[7] Currently, AAV1 is one of the most efficient serotypes for muscle transduction.[8,9]

Received March 25, 2007; first decision April 13, 2007; revision accepted June 22, 2007.

From the Divisions of Genetic Therapeutics (T.I., R.U., M.U., H.M., A.K., K.O.), Cardiovascular Medicine (T.I., H.M., K.S.), and Cell and Molecular Medicine (J.M., Y.S.), Jichi Medical University, Tochigi, Japan; the Department of Molecular Therapy (T.O.), National Institute of Neuroscience, National Center of Neurology and Psychiatry, Tokyo, Japan; and the Department of Organ Regeneration (M.T., U.I.), Shinshu University Graduate School of Medicine, Matsumoto, Japan.

Correspondence to Takayuki Ito or Keiya Ozawa, Division of Genetic Therapeutics, Jichi Medical University, 3311-1 Yakushiji, Shimotsuke, Tochigi 329-0498, Japan. E-mail titou@jichi.ac.jp or kozawa@jichi.ac.jp

Hypertension **is available at http://hyper.ahajournals.org** **DOI: 10.1161/HYPERTENSIONAHA.107.091348**

Single subcutaneous injection of a pyrrolizidine alkaloid, namely, monocrotaline (MCT), produces severe PAH and PA remodeling in rats. We examined the effects of sustained PGIS expression in preventing PAH development and progression by means of this widely used model and an AAV1 vector.

Methods

Western Blot Analysis for PGIS Expression In Vitro

Human embryonic kidney 293 (HEK293) cells were incubated in 10-cm dishes containing DMEM and nutrient mixture F12 (Invitrogen) with 2% FCS in an atmosphere of 5% CO_2 in air at 37°C. The cells at 70% confluence were transfected with an AAV proviral plasmid encoding human PGIS (phPGIS, a kind gift from Dr Mimuro) or plasmid encoding enhanced green fluorescent protein (eGFP) by using a calcium phosphate method. The cells were harvested 72 hours after transfection, and cell lysates were prepared with a lysis buffer (10 mmol/L of Tris-HCl, 150 mmol/L of NaCl, and 1% NP40 [pH 7.6]) containing Complete Mini protease inhibitor (Roche Diagnostics). For Western blot analysis, 10 μg of the lysate was subjected to 10% SDS-PAGE and transferred to a nitrocellulose membrane. The membrane was blocked and incubated with a 1:500 dilution of rabbit anti-human PGIS polyclonal antibody (a gift from Dr Mimuro) and a 1:5000 dilution of peroxidase-linked anti-rabbit IgG antibody (Amersham Pharmacia Biotech), and immunoreactive bands were visualized using an enhanced chemiluminescence Western blotting kit (Amersham).

AAV-PGIS Production and PGI_2 Expression

We developed a recombinant AAV1-based vector containing the human PGIS or eGFP gene controlled by a modified chicken β-actin promoter with a cytomegalovirus immediate-early enhancer (AAV-PGIS or AAV-eGFP) to obtain efficient transgene expression in skeletal muscle cells. The AAV vectors were prepared according to the previously described 3-plasmid transfection adenovirus-free protocol with minor modifications for enabling the use of an active gassing system.[10,11] In brief, 60% confluent HEK293 cells that were incubated in a large culture vessel with active air circulation were cotransfected with phPGIS, AAV-1 chimeric helper plasmid (p1RepCap), and adenoviral helper plasmid pAdeno (Avigen Inc). The crude viral lysate was purified with 2 rounds of cesium chloride 2-tier centrifugation.[12] The titer of the viral stock was determined against plasmid standards by real-time PCR with primers 5′-CCCGCGAGGTTGTGGTGGAC-3′ and 5′-ATGGGCGGATGCGGTAGC-3′; subsequently, the stock was dissolved in a buffer (50 mmol/L of HEPES [pH 7.4] and 0.15 mol/L of NaCl [HN buffer]) before infection. The HEK293 cells cultured in 6-well plates containing DMEM and nutrient mixture F12 with 5% FCS were infected with AAV-PGIS at 1×10^4 genome copies per cell to evaluate PGI_2 expression in vitro, and the supernatant was harvested after 72 hours. Concentrations of 6-keto-prostaglandin $F_{1\alpha}$ (6-keto-$PGF_{1\alpha}$) in plasma or culture media were determined by enzyme immunoassay (R&D Systems) according to the manufacturer's instructions. The minimum detectable dose of the assay was <1.4 pg/mL. Interassay and intra-assay precision of the kit was <10%.

Animal Models

All of the animal experiments were approved by the Jichi Medical University ethics committee and were performed in accordance with the National Institutes of Health Guide for the Care and Use of Laboratory Animals. To evaluate the efficiency of gene expression in vivo, AAV-eGFP (200 μL; 1×10^{11} gene copies per body) or AAV-PGIS (200 μL; 1×10^{10} to 1×10^{11} gene copies per body) was injected into the bilateral anterior tibial muscles (n=3 each) of 3-week–old male Wistar rats (Clea Japan Inc) weighing 45 to 55 g. For hemodynamics and histological analyses, the rats were divided into 4 groups: sham rats that were administered the HN buffer (group 1, negative control [NC] group; n=4); MCT-PAH rats administered the HN buffer (group 2, MCT group; n=6); MCT rats administered AAV-eGFP (group 3, MCT+eGFP group; n=6); and MCT rats administered AAV-PGIS (group 4, MCT+PGIS group; n=10). After the anesthesia with spontaneous inhalation of 1% isoflurane, the rats in groups 3 and 4 were intramuscularly injected with AAV-eGFP or AAV-PGIS (1×10^{10} gene copies per body), whereas those in groups 1 and 2 were injected with the HN buffer (200 μL). MCT (Wako Pure Chemicals) was dissolved in 0.1 N HCl, and the pH was adjusted to 7.4 with 1.0 N NaOH. After the anesthesia with spontaneous inhalation of 1% isoflurane, all of the rats except for those in the NC group were injected subcutaneously with MCT (40 mg/kg) 4 weeks after the injecting the vector. Blood samples were collected from the tail vein on ethylenediamine tetraacetic acid tubes, and the concentrations of the leukocytes, platelets, hematocrit, alanine aminotransferase, and creatinine were determined by standard procedures.

Hemodynamics Analysis

Four weeks after the MCT injection, the rats were anesthetized with spontaneous inhalation of 1% isoflurane, and a tracheotomy was performed. Then, they were mechanically ventilated with 1% isoflurane (tidal volume, 10 mL/kg; respiratory rate, 30 breaths per minute) through a tracheostomy. After the thoracic cavity was opened using a midsternal approach, 2F high-fidelity manometer-tipped catheters (SPC-320; Millar Instruments Inc) were inserted directly into the right or left ventricle, and an ultrasonic flow probe (flow probe 2.5S176; Transonic Systems Inc) was placed on the ascending root of the aorta. The heart rate, mean pulmonary arterial pressure (mPAP), aortic systolic arterial pressure, left ventricular end-diastolic pressure (LVEDP), and mean aortic flow indicating the cardiac output (CO) were measured. Cardiac indices (CI) and pulmonary vascular resistance (PVR) were calculated using the following formula: CI ($mL\cdot min^{-1}\cdot kg^{-1}$)=CO/body weight, PVR ($mm\,Hg\cdot mL^{-1}\cdot min^{-1}\cdot kg^{-1}$)=(mPAP−LVEDP)/CI.

Ventricular Weight Measurement and Morphometric Analysis of the PA

After the hemodynamic analysis, the rats were killed with an overdose (5%) of isoflurane through a tracheostomy. Their lungs were perfused with 5 mL of saline followed by 10 mL of cold 4% paraformaldehyde. Each ventricle and the lungs were then excised, dissected free, and weighed. The weight ratio of the right ventricle to the left ventricle plus septum [RV/(LV+S)] was calculated as an index of right ventricular hypertrophy (RVH). The lung tissues were fixed overnight at 4°C in 4% paraformaldehyde and frozen in Tissue-Tek OCT compound (Sakura Finetechnical Co) at −20°C. Hematoxylin and eosin staining was performed on 7-μm–thick sections that were subsequently examined using light microscopy. A morphometric analysis was performed on a PA having an external diameter of 25 to 50 μm or 51 to 100 μm. The medial wall thickness was calculated using the following formula: medial thickness (%)=medial wall thickness/external diameter×100.[13] For the quantitative analysis, 30 vessels of each rat were measured and averaged randomly by the 2 external observers.

Survival Analysis

The 3-week–old Wistar rats were divided into 3 groups (MCT, MCT+eGFP, and MCT+PGIS; n=8 each). After the anesthesia with spontaneous inhalation of 1% isoflurane, the rats in the MCT+eGFP or MCT+PGIS group were intramuscularly injected with AAV-eGFP or AAV-PGIS at 1×10^{10} genome copies per body, respectively. Under the same anesthetic condition, all of the rats were injected subcutaneously with MCT (40 mg/kg) at 4 weeks after injecting the vector. The survival rate was estimated from the date of the MCT administration until death or after 8 weeks of the injection. Survival curves were analyzed using the Kaplan-Meier method and compared by log-rank tests.

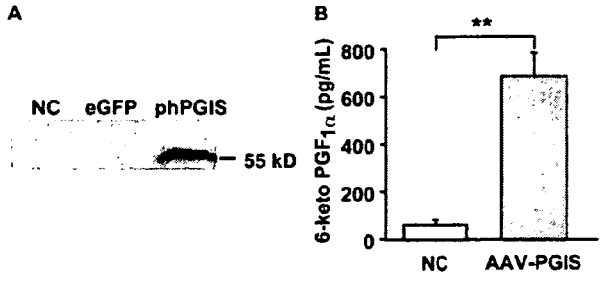

Figure 1. Expression of PGIS and PGI_2 in vitro. A, Western blot analysis of PGIS expression in HEK293 cells after plasmid transfection. The cells were harvested 72 hours after transfection with phPGIS or eGFP. B, AAV vector-mediated PGI_2 expression in HEK293 cells. The PGI_2 levels were estimated by measuring the amount of 6-keto-$PGF_{1\alpha}$, a stable metabolite of PGI_2, in the culture supernatant by enzyme immunoassay 72 hours after infecting the cells (n=4 each) with AAV-PGIS (1×10^4 genome copies per cell). Data are presented as mean±SEM. $^{**}P<0.01$. NC indicates untreated negative control.

Statistical Analysis

The statistical analysis and correlations were performed using StatView (Abacus Concepts, Inc). Data are presented as mean±SEM. Differences in parameters were evaluated using ANOVA combined with Fisher's test. A value of $P<0.05$ was considered statistically significant.

Results

Expression of PGIS and PGI_2 In Vitro

Western blot analysis revealed that transfection of the HEK293 cells with phPGIS but not with a plasmid carrying the eGFP gene enhanced the production of the PGIS protein (Figure 1A). Infection of the cells with AAV-PGIS at 1×10^4 genome copies per cell significantly increased the concentration of 6-keto-$PGF_{1\alpha}$, a stable metabolite of PGI_2, in culture supernatants as compared with that without vector infection (Figure 1B).

AAV Vector-Mediated Systemic PGI_2 Expression in the Rats

Four weeks after the injection of AAV vectors (1×10^{10} genome copies per body), the PGIS-transduced rats began exhibiting significant increases in the plasma 6-keto-$PGF_{1\alpha}$ levels as compared with the control rats (Figure 2A). Eight weeks after the injection, the 6-keto-$PGF_{1\alpha}$ levels increased further in a vector dose-dependent manner in the treated rats (Figure 2B) as compared with the untreated controls (6.68±1.33 versus 1.62±0.30 ng/mL, 1×10^{11} versus 1×10^{10} genome copies per body, respectively; $P<0.05$; n=3 each). The vectors at 1×10^{10} genome copies per body were used for all of the subsequent experiments. In contrast, injection of 1×10^{11} genome copies per body of AAV-eGFP produced no significant change in the 6-keto-$PGF_{1\alpha}$ levels.

Effects of PGI_2 Expression on Hemodynamics and RVH

Four weeks after the MCT administration, the mPAP levels were significantly elevated in the treated rats as compared with the untreated controls (Figure 3A). Treatment with AAV-PGIS but not AAV-eGFP significantly inhibited this increase (Figure 3A). In addition, the expression of PGI_2

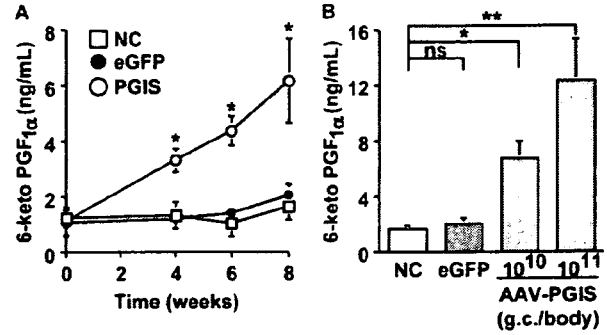

Figure 2. AAV vector-mediated systemic expression of PGI_2 in vivo. The concentration of plasma 6-keto-$PGF_{1\alpha}$ was determined by enzyme immunoassay after a single injection of AAV-PGIS into the anterior tibial muscle of 3-week-old male Wistar rats. A, Time course of plasma 6-keto-$PGF_{1\alpha}$ levels after injection of AAV-PGIS at 1×10^{10} genome copies per body. B, Vector dose dependency of plasma 6-keto-$PGF_{1\alpha}$ levels 8 weeks after the injection. The rats injected with AAV-eGFP (1×10^{11} genome copies per body) were used as controls. Data are presented as mean±SEM (n=3 animals per group). ns indicates not statistically significant; NC, untreated negative control. $^{*}P<0.05$ vs NC; $^{**}P<0.01$.

significantly mitigated an increase in PVR and a decrease in CI that were induced by MCT (Figure 3B and 3C, respectively); however, it produced no significant changes in the heart rate and aortic systolic arterial pressure (Table). PGI_2 expression also had a beneficial effect on RVH. Treatment with AAV-PGIS but not AAV-eGFP significantly inhibited the MCT-induced increase in RV/(LV+S) (Figure 3D).

Effects on Medial Hypertrophy of the PA

Medial hypertrophy is a hallmark of pathological vascular remodeling in PAH. Four weeks after the MCT injection, the

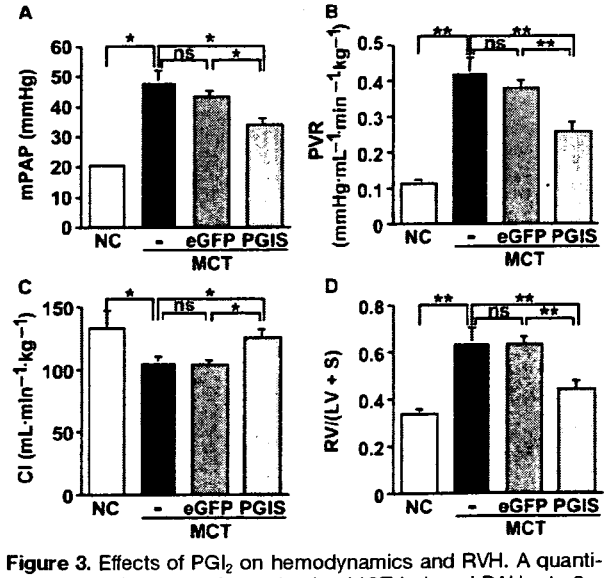

Figure 3. Effects of PGI_2 on hemodynamics and RVH. A quantitative analysis was performed using MCT-induced PAH rats 8 weeks after injecting the vector. A, mPAP (mm Hg); B, PVR (mm Hg · mL^{-1} · min^{-1} · kg^{-1}); C, CI (mL · min^{-1} · kg^{-1}). D, Weight ratio of the right ventricle to the left ventricle plus septum [RV/(LV+S)] presented as an index of RVH. Data are presented as means±SEM (n=4 to 10 animals per group). $^{*}P<0.05$; $^{**}P<0.01$. ns indicates not statistically significant; NC, untreated negative control.

Physiological and Laboratory Data of the MCT-Induced PAH Rats

Factor	NC	MCT	MCT+eGFP	MCT+PGIS	*P*
No. of rats	4	6	6	10	...
Heart rate, per minute	294.0±10.6	281.2±14.7	268.0±9.0	274.8±8.7	NS
ASAP, mm Hg	99.5±1.6	97.3±2.0	96.3±2.4	94.7±4.4	NS
Body weight, g	358.5±11.5	328.3±7.2	328.0±11.4	342.5±9.8	NS
Leukocyte, per mL	6725±372	7917±723	8800±849	8030±852	NS
Hematocrit, %	48.2±0.7	48.9±1.9	51.0±3.0	47.8±1.8	NS
Platelet, $\times 10^4/mm^3$	88.3±8.7	79.2±8.8	80.4±3.6	84.6±6.3	NS
ALT, IU/L	37.8±2.5	49.5±8.4	52.5±6.8	44.1±4.3	NS
Cr, mg/dL	0.52±0.04	0.59±0.05	0.48±0.03	0.53±0.04	NS

Data are presented as means±SEM (n=4 to 10 animals per group). ASAP indicates aortic systolic arterial pressure; ALT, serum alanine aminotransferase; Cr, serum creatinine; NS, not statistically significant.

medial thickness of the PA was greater in the MCT-administered rats than in the untreated controls (Figure 4A). Treatment with AAV-PGIS but not AAV-eGFP prevented the MCT-induced increase in the percentage of medial thickness significantly (Figure 4B, 25 to 50 μm; Figure 4C, 51 to 100 μm in external diameter).

Effects on the Survival of the MCT-PAH Rats and Their Organ Dysfunctions

The PGIS-transduced rats exhibited significantly improved survival rates as compared with the eGFP-transduced rats (Figure 5). The MCT administration produced a slight but not significant decrease in the body weight of the rats, and PGIS gene transfer prevented this decrease. Although the MCT group showed only a slight but not significant increase in the leukocyte count and serum alanine aminotransferase levels as compared with the NC group, the AAV-PGIS treatment caused no additional change in these parameters (Table).

Discussion

The present study demonstrates that sustained PGI_2 expression by a single intramuscular injection of AAV-PGIS prevents the development of MCT-PAH in rats. PGI_2 expression not only increased the cardiac output significantly but also prevented the progression of PVR, RVH, and medial hypertrophy of the PA that was induced by the MCT administration. The PGIS-transduced rats also exhibited significantly improved survival rates as compared with the controls. Furthermore, the PGIS expression observed in this study caused no additional adverse effects on hematologic data and serum indicators of hepatorenal function (alanine aminotransferase and creatinine levels) in the MCT-PAH rats.

The expression of PGI_2 and PGIS decreased in the remodeled PAs of the idiopathic PAH patients.[14,15] Impaired PGI_2 synthesis resulting from a decrease in PGIS expression may be implicated in the pathogenesis of PAH. In fact, continuous intravenous infusion of exogenous PGI_2 markedly lowers PVR and improves survival in PAH patients. However, this system requires lifelong infusion with a central venous catheter because of the short biological half-life of PGI_2. Furthermore, because this system is associated with life-threatening complications (eg, shock and sepsis) that may result in poor survival and quality of life of patients, stable

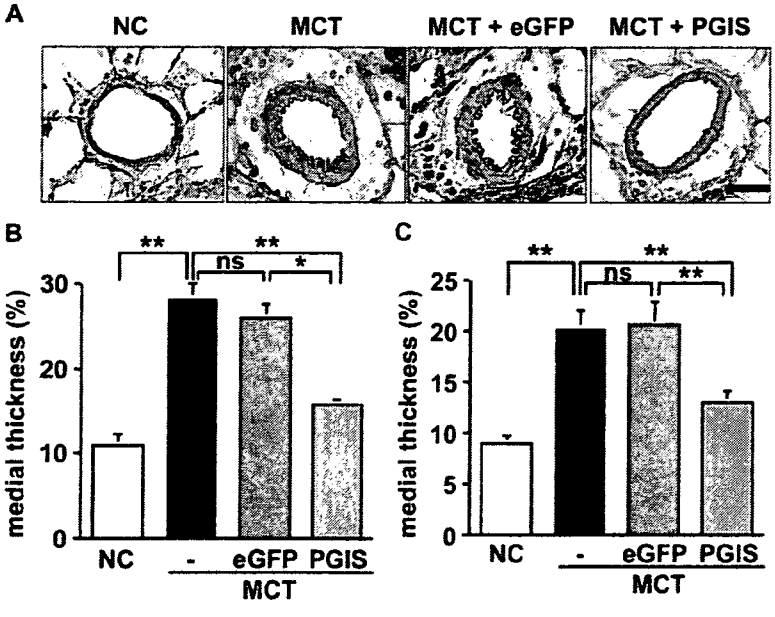

Figure 4. Effects of PGI_2 on medial hypertrophy of the peripheral PA. A, Representative cross-sections of the peripheral PA 4 weeks after the MCT administration (hematoxylin and eosin staining, original magnification, ×1000; scale bar=20 μm). B and C, Quantitative analysis of percentage of medial thickness (B, 25 to 50 μm; C, 51 to 100 μm in external diameter). Data are presented as means±SEM (n=4 to 10 animals per group). *$P<0.05$, **$P<0.01$. ns indicates not statistically significant; NC, untreated negative control.